J. H. LIENHARD

Associate Professor,
Department of Mechanical
Engineering.
Mem. ASME

P. T. Y. WONG

Teaching Assistant, Department
of Mechanical Engineering.

Washington State University,
Pullman, Wash.

The Dominant Unstable Wavelength and Minimum Heat Flux During Film Boiling on a Horizontal Cylinder

Predictions of the dominant unstable wavelength and the minimum heat flux during film boiling above a flat plate are found to be inapplicable in the case of boiling on small wires. New expressions are developed for the case of a horizontal cylinder, by accounting for the effect of surface tension in the transverse direction upon the Taylor instability of the interface.

Original measurements of wavelengths and minimum heat fluxes on small wires are also provided. These data support the predictions.

Introduction

THE film boiling regime is characterized by the steady formation and release of bubbles at the liquid-over-vapor interface over a heating element. Zuber and Tribus [1,2][1] proposed in 1958, that this behavior resulted from the Taylor instability of the liquid-vapor interface. They argued that, as long as more vapor was being generated than was required to sustain the natural rate of growth of unstable disturbances, the disturbances would collapse and release bubbles periodically. It also followed that the spacing between bubbles would be a constant value equal to the wavelength of the disturbance most susceptible to collapse.

Earlier studies of plane unstable interfaces by Kelvin [3], and by Bellman and Pennington [4], provided Zuber and Tribus with expressions for the wavelength, λ_c, of the shortest unstable disturbance, and the wavelength, λ_d, of the most dangerous unstable disturbance. Kelvin showed that all disturbances with wavelengths less than λ_c, where:

$$\lambda_c = 2\pi \left[\frac{\sigma}{g(\rho_f - \rho_g)} \right]^{1/2} \tag{1}$$

would be stable. Bellman and Pennington showed that disturbances would grow most rapidly when:

$$\lambda_d = 2\pi \left[\frac{3\sigma}{g(\rho_f - \rho_g)} \right]^{1/2} \tag{2}$$

The term σ in equations (1) and (2) designates the surface ten-

---

[1] Numbers in brackets designate References at the end of paper.
Contributed by the Heat Transfer Division of THE AMERICAN SOCIETY OF MECHANICAL ENGINEERS and presented at the ASME-AIChE Heat Transfer Conference and Exhibit, Boston, Mass., August 11–14, 1963. Manuscript received at ASME Headquarters, March 12, 1963. Paper No. 63—HT-3.

sion between a liquid and its vapor; ρ_f and ρ_g are the liquid and vapor densities, respectively; and g is the gravitational acceleration.

Zuber [2] predicted the minimum boiling heat flux with the aid of an experimental result given by Lewis [5]. Lewis found that the initially exponential rate of growth of unstable disturbances predicted by Taylor [6] applied in the range of $0 \leq \eta \leq 0.4\lambda$, where η is the ordinate of the disturbance. Accordingly, Zuber fixed q_{min} as the lowest heat flux which generated enough vapor to give rise to the theoretical value of the average $d\eta/dt$ in this range.

The minimum boiling heat flux, q_{min}, obtained in this manner is:

$$q_{min} = \frac{\pi^2}{60} \sqrt[4]{\frac{4}{3}} \; \rho_g h_{fg} \sqrt[4]{\sigma g \frac{\rho_f - \rho_g}{(\rho_f + \rho_g)^2}} \tag{3}$$

where h_{fg} is the latent heat of vaporization. Equation (3) is successful in predicting q_{min} for a flat plate, but recent experiments (e.g. [7]) have shown that q_{min} values for slender horizontal wires are considerably higher than the flat plate value. The present study was thus motivated by a need to know what factors govern the failure of flat plate theory in describing boiling upon cylindrical heaters.

Prediction of the Unstable Wavelengths

The geometry of the liquid-vapor interface surrounding a wire during film boiling will be assumed to take a sinusoidally undulating, asymmetrical form as shown in Fig. 1. The vapor blanket surrounding the heater will be assumed to be sufficiently thin that the smallest radius of the interface is negligibly larger than the radius, R, of the heater. The maximum perturbing amplitude, a, of the dominant wave will occur at the top of the interface. The problem of deciding whether the dominant wave-

Nomenclature

a = maximum amplitude of an interfacial wave
g = gravitational acceleration
h_{fc} = latent heat of vaporization
k = wave number, $2\pi/\lambda$
k_c, k_d = wave numbers based upon λ_c and λ_d, respectively
p = pressure
p_g, p_f = pressures at vapor-liquid interface in the vapor and liquid phases, respectively
p_t = effect of transverse surface tension in terms of pressure at the interface

Δp_t = oscillating component of p_t
q = heat flux
q_{min} = minimum film boiling heat flux
R = radius (in particular, the radius of a heating element)
R_b = radius of a departing bubble
R_1 = radius of interface in the x-y plane
t = time
x = distance on axis of heater
y = distance upward from the average (or undisturbed) ordinate of the interface

η = ordinate of interface
λ = wavelength (in particular, the dominant wavelength during film boiling)
λ_c, λ_d = the "critical" and "most dangerous" wavelengths, respectively
ρ_f, ρ_g = densities of saturated liquid and saturated vapor, respectively
σ = surface tension between a liquid and its vapor
ω = angular frequency
ω_{max} = the maximum imaginary value of ω
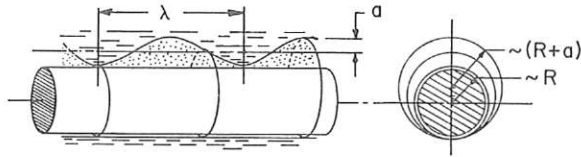
Fig. 1 The assumed geometry of film boiling on a horizontal cylindrical heater

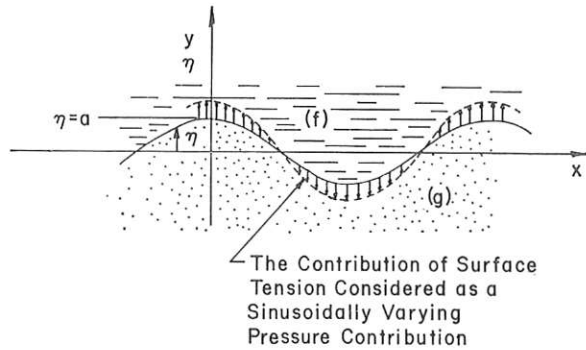The Contribution of Surface Tension Considered as a Sinusoidally Varying Pressure Contribution

Fig. 2 Two-dimensional model for film boiling on a horizontal cylindrical heater

length, λ, should be equal to the critical or the most dangerous wavelength will be deferred until later.

The effect of surface tension along the curvature in the transverse direction is the same as an additional component of pressure, p_t, acting to push the interface in toward the wire, where:

$$p_t = \frac{\sigma}{\text{radius}} \quad (4)$$

this "pressure" ranges between σ/R in the valleys and $\sigma/(R + a)$ at the peaks of the wave; it has an average value of $\sigma / \left(R + \dfrac{a}{2} \right)$ and an amplitude of $\sigma a/2(R^2 + aR)$. The amplitude can be approximated as $\sigma a/2R^2$ since $R \gg a$. This pressure contribution will act in phase with the collapsing wave and will serve to shorten the dominant wavelength.

A simplified two-dimensional analytical model will be established to describe this three-dimensional physical model. Fig. 2 shows an equivalent two-dimensional wave in a liquid-over-vapor interface. The contribution of curvature in the transverse direction will be included in the form of an additional pressure difference component, Δp_t, across the interface. This component will be numerically equal to the oscillating component of p_t.

The analytical description of this model is built upon the work of Rayleigh and Kelvin (as described by Lamb [3]) as follows:

The interface is assumed to be disturbed by waves of the form:

$$\eta = a \cos kx \cos \omega t \quad (5)$$

which, when ω is real, is to be construed as the real part of:

$$\eta = a e^{-i\omega t} \cos kx \quad (6)$$

where ω is the angular frequency of the wave and the wave number, k, is:

$$k = \frac{2\pi}{\lambda} \quad (7)$$

The liquid and vapor are assumed to be incompressible and inviscid, and the perturbation is assumed to be small in comparison with the depth of both fluid layers. Bernoulli's equation for the system is then:

$$p_g - p_f = a \cos kx \cos \omega t \left[(\rho_f + \rho_g)\frac{\omega^2}{k} + (\rho_f - \rho_g)g \right] \quad (8)$$

The pressure difference $(p_g - p_f)$, which balances the inertia terms on the right-hand side of equation (8) is composed of two parts:

$$p_g - p_f = -\Delta p_t - \frac{\sigma}{R_1} \quad (9)$$

where Δp_t, being in phase with the disturbance, is:

$$\Delta p_t = \frac{\sigma}{2R^2} a \cos kx \cos \omega t \quad (10)$$

and $1/R_1$, the inverse radius of curvature in the x-y plane, is:

$$\frac{1}{R_1} = \frac{\partial^2 \eta}{\partial x^2} = -ak^2 \cos kx \cos \omega t \quad (11)$$

Substitution of equations (10) and (11) into equation (9), and of the result into equation (8) gives:

$$(\rho_f + \rho_g)\frac{\omega^2}{k} + (\rho_f - \rho_g)g = \sigma k^2 - \frac{\sigma}{2R^2} \quad (12)$$

or:

$$\omega^2 = -kg\frac{\rho_f - \rho_g}{\rho_f + \rho_g} + \frac{\sigma k^3}{\rho_f + \rho_g} - \frac{\sigma k}{2(\rho_f + \rho_g)R^2} \quad (13)$$

The nature of ω governs the stability of the disturbance (as Taylor [6] has shown). If ω is real, the stabilizing effect of surface tension in the axial direction will smooth out the disturbance. If ω is imaginary, the forces of gravity and surface tension in the transverse direction will dominate and the disturbance will increase exponentially, in accordance with equation (6).

In the present case, ω passes from real to imaginary as the right-hand side of equation (13) passes through zero. The critical wave number, k_c, is then obtained by equating the right-hand side to zero:

$$k_c = \sqrt{\frac{g(\rho_f - \rho_g)}{\sigma} + \frac{1}{2R^2}} \quad (14)$$

and the critical wavelength:

$$\lambda_c = \frac{2\pi}{\sqrt{\dfrac{g(\rho_f - \rho_g)}{\sigma} + \dfrac{1}{2R^2}}} \quad (15)$$

The most dangerous wave number, k_d, is obtained by maximizing $(-i\omega)$:

$$\left[\frac{d(i\omega)}{dk} \right]_{k=k_d} = \left[\frac{d}{dk} \left(kg\frac{\rho_f - \rho_g}{\rho_f + \rho_g} - \frac{\sigma k^3}{\rho_f + \rho_g} + \frac{\sigma k}{2(\rho_f + \rho_g)R^2} \right)^{1/2} \right]_{k=k_d} = 0 \quad (16)$$

whence:

$$k_d = \frac{1}{\sqrt{3}} \sqrt{\frac{g(\rho_f - \rho_g)}{\sigma} + \frac{1}{2R^2}} \quad (17)$$

and:

$$\lambda_d = \frac{2\pi \sqrt{3}}{\sqrt{\dfrac{g(\rho_f - \rho_g)}{\sigma} + \dfrac{1}{2R^2}}} \quad (18)$$

Equations (15) and (18) show that as R is decreased, surface tension in the transverse direction acts to shorten the wavelength. The wavelength will, in fact, diminish in direct proportion to the radius when:

$$R \ll \sqrt{\frac{\sigma}{2g(\rho_f - \rho_g)}}$$

Prediction of the Minimum Heat Flux

A minimum heat flux prediction for the present configuration can now be formed with the help of an energy balance at the surface of the heater:

$$q_{min} = \begin{bmatrix} \text{latent heat} \\ \text{transport} \\ \text{per bubble} \end{bmatrix} \begin{bmatrix} \text{bubbles} \\ \text{per wave} \\ \text{oscillation} \end{bmatrix}$$

$$\begin{bmatrix} \text{minimum number} \\ \text{of oscillations} \\ \text{per unit time} \end{bmatrix} \begin{bmatrix} \text{waves per} \\ \text{unit area} \\ \text{of heater} \end{bmatrix} \quad (19)$$

or:

$$q_{min} = \left[\rho_g h_{fg} \frac{4\pi}{3} \left(\frac{\lambda_d}{4} \right)^3 \right] [2] \left[\frac{1}{\lambda_d} \frac{\overline{d\eta}}{dt} \right] \left[\frac{1}{2\pi R \lambda_d} \right] \quad (20)$$

where, with aid of equation (6):

$$\frac{\overline{d\eta}}{dt} = \frac{1}{0.4\lambda_d} \int_0^{0.4\lambda_d} \frac{d\eta}{dt} \, d\eta = 0.2\lambda_d(i\omega_{max}) \quad (21)$$

Equation (20) is a direct adaptation of Zuber's q_{min} derivation. Three of his assumptions are also being employed tentatively in the case of a cylindrical heater. These assumptions are tested in the subsequent sections of this paper:

1 The dominant wavelength is λ_d.
2 The departure radius of a bubble is $\lambda_d/4$.
3 Lewis' experimental determination of the range in which the wave grows exponentially applies in the present configuration.

Substitution of equations (21), (13), and (18) into equation (20) yields the desired prediction for q_{min}:

$$q_{min} = \frac{\pi^2}{60} \sqrt[4]{3} \frac{\rho_g h_{fg}}{R} \left[2g \frac{\rho_f - \rho_g}{\rho_f + \rho_g} \right.$$
$$\left. + \frac{\sigma}{(\rho_f + \rho_g)R^2} \right]^{1/2} \left[\frac{g(\rho_f - \rho_g)}{\sigma} + \frac{1}{2R^2} \right]^{-3/4} \quad (22)$$

Experimental Determination of the Dominant Wavelength and q_{min}

A program of experimental evaluations of λ and q_{min} on slender horizontal wires has been made in order to test the preceding predictions. Resistance wires of Nichrome V ($0.0025 \leq R$ in. ≤ 0.0254) and Tungsten ($0.001 \leq R$ in. ≤ 0.002) were mounted in a horizontal pyrex tube at atmospheric pressure and used to boil isopropanol and benzene of reagent grade. The apparatus, shown in Fig. 3, embodied the following features:
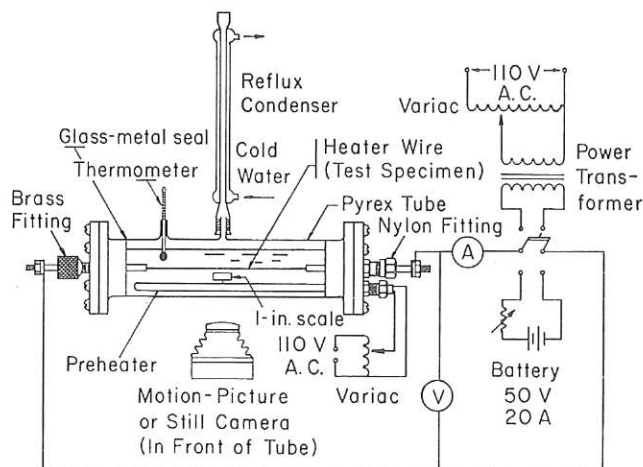

Fig. 3 Schematic representation of experimental apparatus

The tubular test section was provided with a thermometer to confirm that the liquid was saturated during runs, and was equipped with a 110V-3A, a-c resistance preheater. A Nichrome rectangle one in. wide was mounted in the same perpendicular plane as the wire to facilitate measurement from photographs. The lighter wires used ($0.001 \leq R$ in. ≤ 0.010) were provided with battery-supplied direct current, while the heavier wires ($0.0159 \leq R$ in. ≤ 0.0254) were, for convenience, supplied with alternating current. Since experimental results were similar for wires of 0.0079-in. radius, upon which observations were made with both a-c and d-c power supplies, the effect of current alternation in the larger wires was judged to be negligible.

Both still and motion pictures were made of the wave action. High-speed (2500 frames per sec) motion pictures were made for benzene boiling on a 0.079-in. radius wire and for isopropanol boiling on wires of 0.0254, 0.0079, and 0.0032 in. radii. Most of the visual data, however, were obtained from a large number of still photographs. Both kinds of visual results consisted strictly of elevation views of the wire during film boiling at heat fluxes in excess of q_{min}.

The test wires were cleaned with soap and hot water, and were rinsed with both hot water and acetone, prior to their installation in the tube. During the experimental runs care was exercised to keep the wires from becoming red hot. This precaution protected both the wire surface and the liquid from deterioration. The preheater was turned off immediately before observations for two reasons. The first was to clear the field of vision of bubbles. The second was to avoid the effect of an electric field (reported by Bonjour et al. [8] in 1962) upon boiling. The field created by the preheater in the present experiments was found to increase q_{min} on the smaller wires by a factor of as much as four.

Heat fluxes were computed directly from measurements of voltage and amperage and the dimensions of the wire. Wavelengths were measured from still photographs or from projections of the 16 mm high-speed motion picture film onto a microfilm-reader screen. The probable error in heat fluxes due to measurements was not over 3 percent in any instance. The probable error in measurements of the wavelengths ranged between 1 percent for the largest one to 20 percent for the smallest.

While the experimental errors were relatively low, somewhat larger errors of judgment arose in observing the minimum heat fluxes and wavelengths. The observation of q_{min} was made difficult by heat conduction into the electrodes which held the wires. This caused film boiling to collapse at the ends at heat fluxes in excess of q_{min}—a difficulty which was overcome by watching for evidence of local collapse away from the ends. The range of uncertainty of interpretation of this observation was about ± 20 percent on the average.[2]

The observation of the dominant wavelength was relatively straightforward for wires for which $R \geq 0.010$ in. The bubble release patterns were generally good although both isolated deformities, and drift in the phase angle of oscillation along the length of the wires, acted to upset the uniformity of the patterns. Fig. 4(a) shows a typical uniform release pattern, and Fig. 4(b) shows typical deformities. The uncertainty of interpretation of wavelength observations in this range was usually about ± 20 percent.

In the case of wires with radii for which $0.0010 \leq R$ in. ≤ 0.010, the phenomenon of bubble merger entered to obscure the wave pattern. Bubbles generated during the first half of a cycle tarried on the wire long enough to come into contact with neighboring bubbles from the second half of a cycle. A merger would occur between the two, which made identification of the local wave pattern impossible. A single instance of this behavior is shown in Fig. 4(c) for a comparatively large wire. Fig. 4(e), on the other hand, shows a small diameter wire on which the wave action can only be observed in a few isolated locations. The average

---

[2] The specific uncertainties of each of the present data are displayed in the graphical presentations of these data.

a) GOOD BUBBLE DEPARTURE. BUBBLES VERY NEARLY IN PHASE WITH ONE ANOTHER. (R = 0.0254 IN., q = 16,000 BTU/FT² HR, ISOPROPANOL)

b) TYPICAL IMPERFECT WAVE PATTERN. (R = 0.0254 IN., q = 16,000 BTU/FT² HR, ISOPROPANOL)

c) GOOD BUBBLE DEPARTURE PATTERN WITH ONE CLEAR CASE OF MERGER. (R = 0.0079 IN., q = 56,000 BTU/FT² HR, BENZENE)

d) RELATIVELY CONTINUOUS PHASE SHIFT ALONG THE LENGTH OF THE WIRE. (R = 0.0079 IN., q = 54,000 BTU/FT² HR, ISOPROPANOL)

e) EXTENSIVE MERGING OF NEIGHBORING BUBBLES. DOMINANT WAVE LENGTHS ARE IDENTIFIED IN TWO PLACES. (R = 0.0032 IN., q = 118,500 BTU/FT² HR, ISOPROPANOL)

f) WAVE BEHAVIOR COMPLETELY OBSCURED BY BUBBLE MERGINGS. (R = 0.0005 IN., q = 450,000 BTU/FT² HR, ISOPROPANOL)
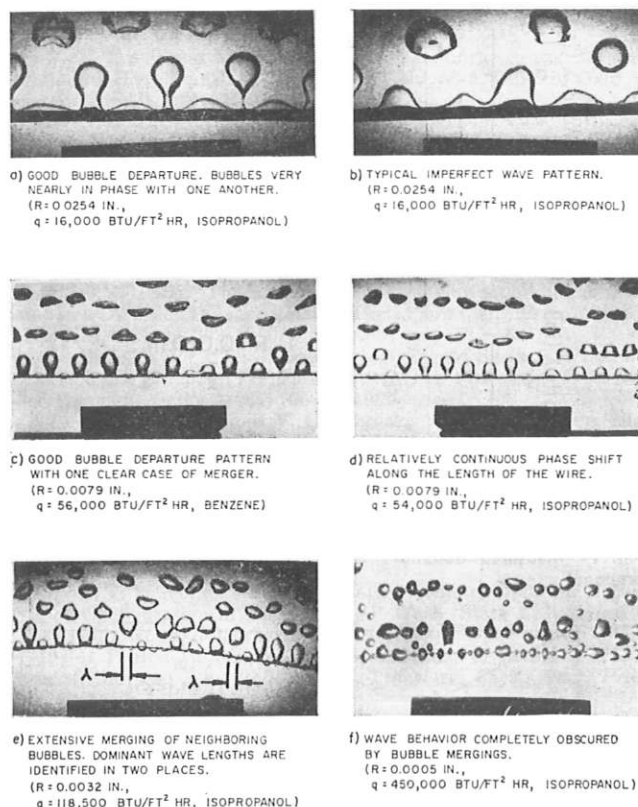
Fig. 4 Various patterns of bubble departure from horizontal wires (black object below wire is 1-in. reference scale)

Table 1 Measured dominant wavelengths and heat fluxes, for various wire sizes and fluids

Liquid	heater radius	dominant wave length	heat flux
	in.	in.	Btu/ft²hr
Isopropanol	0.0010	0.021	144,000
	0.0015	0.029	61,000
	0.0020	0.036	45,000
	0.0025	0.048	52,000
	0.0032	0.060	60,000
	0.0050	0.112	31,000
	0.0063	0.126	36,000
	0.0079	0.155	17,200
	0.0100	0.200	14,300
	0.0159	0.288	12,000
	0.0201	0.341	16,700
	0.0254	0.450	16,400
Benzene	0.0015	0.033	112,900
	0.0020	0.048	50,000
	0.0025	0.066	45,600
	0.0040	0.068	54,000
	0.0050	0.118	19,100
	0.0079	0.173	19,700
	0.0100	0.193	17,400

Table 2 Measured dominant wavelengths for various heat fluxes for isopropanol

heater radius	heat flux	dominant wave length
in.	Btu/ft²hr	in.
0.0025	47,500	0.052
	52,000	0.048
	66,000	0.048
	76,500	0.046
	82,000	0.049
	89,500	0.050
	93,600	0.048
	103,000	0.049
	131,000	0.051
	171,000	0.050
0.0100	14,300	0.200
	15,500	0.194
	20,100	0.197
	22,500	0.209
	26,100	0.203
	30,200	0.207
	39,800	0.209
	50,000	0.218

Table 3 Measured minimum heat flux for various wire sizes for isopropanol

heater radius (in.)	q_{min} (Btu/ft²hr)
0.0025	21,500
0.0032	22,500
0.0050	16,600
0.0063	15,500
0.0100	12,500
0.0159	8,200
0.0254	6,600

Table 4 Measured bubble radii and the ratio of λ/R_b for various wire sizes for isopropanol

heater radius	bubble radius	λ/R_b	nature of wave pattern
in.	in.	–	–
0.0063	(0.040)	(3.3)	serious merging
0.0079	(0.045)	(3.5)	some merging
0.0100	0.055	3.6	little
0.0159	0.0700	4.1	or
0.0201	0.0900	3.8	no
0.0254	0.1000	4.5	merging

Table 5 Range of amplitude during which interface grows exponentially

Liquid	heat flux	heater radius	range of exponential growth, and uncertainty of observation
	Btu/ft²hr	in.	
Benzene	56,000	0.0080	$0 \leq \eta \leq 0.53\lambda$ (±10%)
Isopropanol	16,000	0.0254	$0 \leq \eta \leq 0.36\lambda$ (±15%)

uncertainty of wavelength observations in this range rose to about ± 40 percent.

No wave action could be identified on wires for which $R < 0.001$ in. Fig 4(f) illustrates this.

Observed wavelengths for the range of radii, and for the two liquids, are presented in Table 1. The heat fluxes at which these observations were made are included as well. Since these heat fluxes are in excess of q_{min}, an additional set of measurements of q and λ for given wires was made to confirm the independence of λ and q. These data are given in Table 2. Table 3 shows the minimum heat flux as a function of radius.

Two additional observations were made to check the second and third assumptions listed above equation (22). Bubble departure radii, R_b, were obtained from the photographs and the ratio λ/R_b was formed (see Table 4). The observations of R_b

were quite reproducible, so the uncertainty of λ/R_b is roughly the same as that of λ. The range of exponential growth of waves was obtained from measurements of a few waves in each of two motion pictures as well (see Table 5).

For a much more detailed description of the present experiments and of data reduction techniques, the reader can consult reference [9].

Comparison of Theory With Experiment

Figs. 5 and 6 display the observed wavelengths for isopropanol and benzene, respectively. Equations (15) and (18)—the theoretical predictions for λ_c and λ_d—are included in these presentations. The data indicate that the dominant wavelength is generally only about 25 percent higher than the predicted λ_d. Furthermore, no dominant wavelength as small as λ_c was ob-
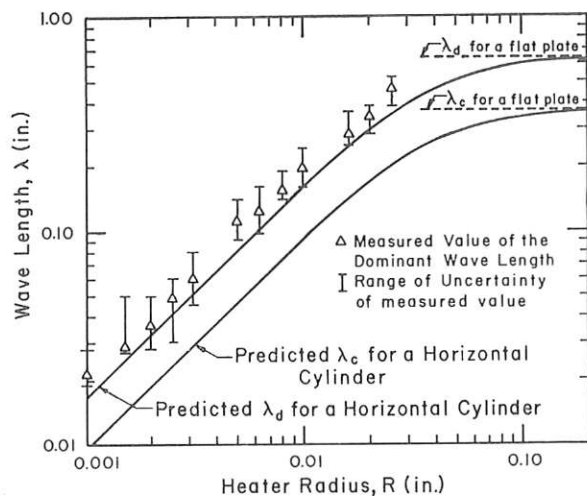
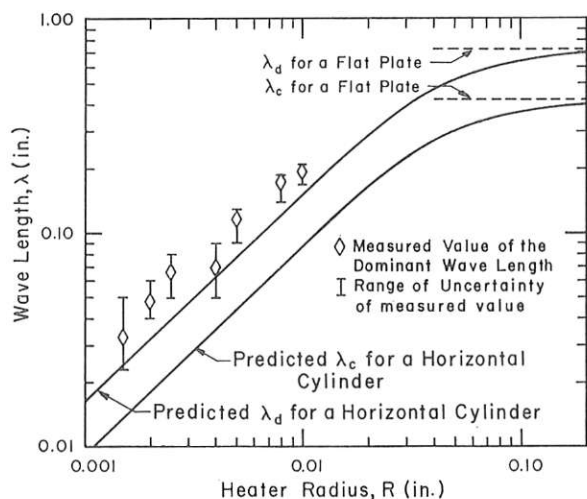**Fig. 5** The effect of heater radius upon the critical and most dangerous wavelengths for isopropanol

Fig. 6 The effect of heater radius upon the critical and most dangerous wavelengths for benzene

Fig. 7 Measured dominant wavelengths versus heat flux for isopropanol

Fig. 8 The effect of heater radius upon q_{min}

served. This suggests that the first assumption in the derivation of equation (22) was correct, and that the present theory is successful. Fig. 7 is included to show that λ can be evaluated at any reasonably low heat flux in excess of q_{min}. The figure shows that there is no identifiable variation of λ with q.

Fig. 8 compares the present q_{min} data with predicted values given by equation (22). Equation (22) predicts that q_{min} will decrease in inverse proportion with R, as R becomes large, since the single row of bubbles will subtend an increasingly large area. Actually, when R becomes large, additional rows of bubbles will be accommodated[3] along the top and the present description will cease to apply.

While Zuber's flat plate prediction does not represent the limit to which equation (22) tends, nor does it describe the physical circumstances of boiling on a large cylinder, it is nevertheless instructive to consider it in Fig. 8. It has therefore been included and with it is shown Berenson's [11] modification of Zuber's prediction. The latter differs from equation (3) only in that the constant $\frac{\pi^2}{60}\left(\frac{4}{3}\right)^{1/4}$ (or 0.177) has been adjusted by semi-empirical means to 0.09.[4] Berenson's prediction accordingly

[3] Breen and Westwater [10] have observed that this two-dimensionality is pronounced in isopropanol boiling on a cylinder of radius, $R = 0.336$ in.

[4] Zuber himself [2] gave an alternate evaluation of the bubble release frequency which indicated that the constant should lie between 0.194 and 0.255.
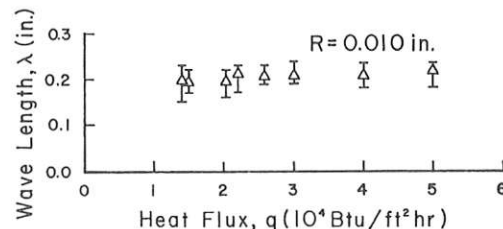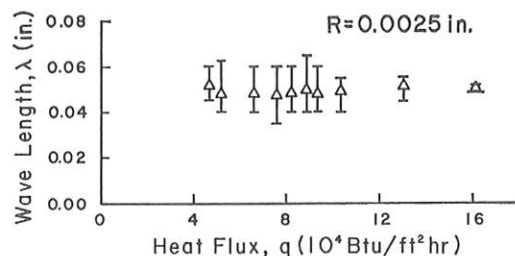
fit his experimental data quite closely. Equation (22) (which is a Zuber-like prediction) would also fit the present data closely if the multiplying constant were arbitrarily reduced from $\frac{\pi^2}{60}\sqrt[4]{3}$ (or 0.216) to a value of 0.057.

It then remains to question the appropriateness of the second and third assumptions used in deriving equation (22). Table 4 shows that the use of $\lambda/4$ as the departure radius is entirely reasonable in the range for which these data can be obtained and Table 5 provides two approximate verifications of the assumed range of exponential growth.

Conclusions

Equation (18) predicts dominant wavelengths during film boiling on a horizontal wire that are 25 percent or less in excess of measured values. It reveals a hitherto unreported decrease in wavelength with heater radius, resulting from the contribution of transverse surface tension.

Zuber's prediction of the minimum heat flux on a flat plate is adapted to the present geometry and the assumptions used in this derivation are supported with experimental data. The resulting prediction is high by a constant factor, as was Zuber's flat plate prediction, although the form of both predictions is apparently correct.

References

1 N. Zuber and M. Tribus, "Further Remarks on the Stability of Boiling Heat Transfer," UCLA Rept. No. 58-5, Univ. of Calif. at Los Angeles, January, 1958.

2 N. Zuber, "Hydrodynamic Aspects of Boiling Heat Transfer," Atomic Energy Commission Report No. AECU-4439, Physics and Mathematics, June, 1959.

3 H. Lamb, *Hydrodynamics*, 6th edition, Dover Publications, New York, N. Y., 1945, p. 455, et. seq.

4 R. Bellman and R. H. Pennington, "Effects of Surface Tension and Viscosity on Taylor Instability," *Quar. Appl. Math.*, vol. 12, 1954, p. 151.

5 D. J. Lewis, "The Instability of Liquid Surfaces When Accelerated in a Direction Perpendicular to Their Planes, II," *Proc. Roy. Soc.* (London), Series A-202, 1950, p. 81.

6 G. I. Taylor, "The Instability of Liquid Surfaces When Accelerated in a Direction Perpendicular to Their Planes, I," *Proc. Roy. Soc.* (London), Series A-201, 1950, p. 192.

7 J. H. Lienhard and V. E. Schrock, "The Effect of Pressure, Geometry, and the Equation of State Upon the Peak and Minimum Boiling Heat Flux," JOURNAL OF HEAT TRANSFER, TRANS. ASME, Series C, vol. 85, p. 261.

8 E. Bonjour, J. Verdier, and L. Weil, "Improvement of Heat Exchanges in Boiling Liquids Under the Influence of an Electric Field," AIChE Preprint 7, AIChE-ASME, 5th Nat'l Heat Transfer Conference, Houston, Texas (August 5 to 8, 1962).

9 P. T. Y. Wong, "Effects of Heater Geometry Upon the Liquid-Vapor Configuration in Film Boiling," Wash. State Univ., Inst. of Tech., Bull. No. 267, February, 1963.

10 B. P. Breen and J. W. Westwater, "Effect of Diameter of Horizontal Tubes on Film Boiling Heat Transfer," *Chem. Engr. Prog.*, vol. 58, no. 7, July, 1962, p. 67.

11 P. J. Berenson, "Transition Boiling Heat Transfer From a Horizontal Surface," M.I.T., Heat Transfer Laboratory Technical Rept. No. 17, 1960.